Mathematical Biology

CrossMark

Effect of light on the growth of non-nitrogen-fixing and nitrogen-fixing phytoplankton in an aquatic system

Gail S. K. Wolkowicz[1] · Yuan Yuan[2]

Abstract We discuss a mathematical model of growth of two types of phytoplankton, non-nitrogen-fixing and nitrogen-fixing, that both require light in order to grow. We use general functional responses to represent the inhibitory effect their biomass has on the exposure to light. We give conditions for the existence and local stability of all of the possible steady-states (die out, single species survival, and coexistence). We derive conditions for global stability of the die out and single-species steady-states and for persistence of both species when the coexistence steady-state exists. Numerical investigation illustrates the qualitative dynamics demonstrating that even under constant environmental conditions, both stable intrinsic oscillatory behavior and a period doubling route to chaotic dynamics are possible. We also show that competitor-mediated coexistence can occur due to the positive feedback resulting from recycling by the nitrogen-fixing phytoplankton. To show the impact of seasonal change in water depth, we also allow the water depth to vary in an annual cycle and discuss echo blooms in this context.

✉ Yuan Yuan
   yyuan@mun.ca

   Gail S. K. Wolkowicz
   wolkowic@mcmaster.ca

[1] Department of Mathematics and Statistics, McMaster University, Hamilton, ON L8S 4K1, Canada

[2] Department of Mathematics and Statistics, Memorial University of Newfoundland, St. John's, NL A1C 5S7, Canada

1 Introduction

Phytoplankton play an important role in aquatic ecosystems as they generate most of the oxygen that we breath. This population growth can be rapid, and typically occur when temperature and nutrient levels rise, usually in late spring and autumn. This rapid growth is commonly referred to as an "algal bloom". Algal blooms occur in freshwater as well as marine environments. While blooms can provide more food to organisms higher up the food chain, too much phytoplankton can also do harm. Dissolved oxygen becomes rapidly depleted as the phytoplankton die, sink to the bottom and decompose. This can result in the death of other organisms including shellfish, crabs, and certain fish.

Nutrient and light are two fundamental resources required for the growth of phytoplankton (Chapin et al. 2011; Passarge et al. 2006). An increase in either nutrient or light can help to overcome limitation by the other. How nutrient availability and light intensity interact to affect aquatic ecosystem dynamics is an interesting question. Attempts to explain patterns in the abundance of phytoplankton in ocean or lakes have usually focused on the supply of limiting nutrients and on grazing pressure by zooplankton (Kolokolnikov et al. 2009; Ruan 1993, 2001; Sarnelle 1992; Watson et al. 1996; Yuan 2012). The role of light has received far less consideration (Huisman and Weissing 1994; Huisman and Weissing 1995; Kunz and Diehl 2003).

Observations from geochemical studies show that nitrate is often a limiting nutrient, where as nitrogen is usually in ample supply. Numerous studies have shown deficiencies in nitrogen inputs relative to outputs in several ocean basins (Bates et al. 1996; Gruber and Sarmiento 1997; Hood et al. 2001; Karl et al. 1992; Michaels et al. 1996; Sambrotto et al. 1993). Biological nitrogen fixation is a biochemical process which can provide a remarkable new nitrogen supply in marine ecosystems (Falkowski 1997; Karl et al. 1997; LaRoche and Breitbarth 2005; Vitousek and Howarth 1991). Trichodesmium is the most prominent planktonic marine nitrogen fixer that uses atmospheric nitrogen directly and converts it to nitrate. Measurement in the tropical North Atlantic, Arabian Sea, and Eastern Indian Ocean show nitrogen fixation by Trichodesmium matches or exceeds nitrate flux into the upper water column, and short-time inputs of new nitrogen from Trichodesmium blooms may be responsible for initiating harmful algal blooms in the Gulf of Mexico (Capone et al. 1997; Carpenter and Romans 1991; Coles et al. 2004; Monteiro and Follows 2009; Olascoaga et al. 2005. The nitrogen-fixing Trichodesmium face numerous competitors that are often faster growing, non-fixing phytoplankton species (Agawin et al. 2007). Studies (Bell et al. 1999) of parts of the Great Barrier Reef Lagoon (a shallow body of water in Australia) have shown that in some sections, although Trichodesmium com-

pete with the non-nitrogen-fixing diatom, new nitrogen produced by Trichodesmium promoted growth of the other phytoplankton species and increased the final eutrophication. Therefore it is essential to understand the interactions between nitrogen-fixing and non-nitrogen-fixing phytoplankton species, and how these are influenced by environmental variations in the ecosystems.

There are many coupled physical-biological models used to study the interactions of Trichodesmium with other phytoplankton. Hood et al. (2001) introduced a six compartment ecosystem model where the growth of Trichodesmium is controlled by light and Trichodesmium competes for light with other non-nitrogen-fixing phytoplankton. Then Trichodesmium pumps nitrogen into the system stimulating growth of other phytoplankton; Later, in (Coles et al. 2004), this ecosystem model was embedded in a 3-dimensional circulation model of the Atlantic ocean (45°N–20°S). This model was able to reproduce the general characteristics of Trichodesmium biomass distribution and generate sequential blooms including secondary or "echo blooms" in a single season. In both Coles et al. (2004), Hood et al. (2001), the authors mainly provide numerical simulations based on the field data. Boushaba and Pascual (2005) introduced a simpler 3-compartment model that includes two types of phytoplankton and involves nonlinear interactions. Their mathematical analysis, showed that the model was able to capture the essential features of larger model in Hood et al. (2001).

In this manuscript, we generalize the simpler model in Boushaba and Pascual (2005) slightly, provide a more complete analysis based on two general functional responses, investigate the role of the mixed-layer depth comparing constant versus seasonally fluctuating, use a bifurcation approach to show that the model admits interesting dynamics that was not reported in Boushaba and Pascual (2005), including the possibility of chaotic dynamics.

The manuscript is organized as follows. We introduce the mathematical model in Sect. 2, and provide a qualitative analysis of the model in Sect. 3, including the existence of the different possible steady-states and their local and global stabilities. We also prove uniform persistence when the coexistence equilibrium exists. In Sect. 4 we present the results of numerical investigation to complement the theoretical predictions, including numerical continuation of invariant sets and numerical simulations. In addition, we investigate the influence of the seasonal fluctuation of water depth on the dynamics. Finally we summarize our results and discuss their ramifications in Sect. 5.

2 Mathematical model

We study a mathematical model in order to explore how nutrient availability and light intensity interact to affect the dynamics of an aquatic ecosystem in which two types of phytoplankton, non-nitrogen-fixing and nitrogen-fixing compete. We model an open system in which nutrients are supplied from an external source (e.g., terrestrial runoff) and/or from turn over from water from deep layers. We assume the water column is well-mixed with depth h measured from zero at the surface to a maximum depth H at the bottom of the water column. Since the water column is well-mixed, we assume that the phytoplankton and nutrients are distributed homogeneously. Only the growth of the non-nitrogen-fixing phytoplankton is assumed to depend on the nutrient availability.

However, we assume that the two types of phytoplankton also compete for light, which is assumed to be more intense at the surface.

In particular, we consider the following model which describes how the concentration of the non-nitrogen-fixing phytoplankton population, $P(t)$, the nitrogen-fixing population Trichodesmium, $T(t)$, and the nutrient, $N(t)$ change as time, t changes.

$$
\begin{aligned}
P' &= P\left(\mu_1 G(P,T)U(N) - \left(d_1 + \frac{D+s_1}{H}\right)\right) \\
T' &= T\left(\mu_2 G(P,T) - \left(d_2 + \frac{D+s_2}{H}\right)\right) \\
N' &= \frac{D}{H}(N^0 - N) - \mu_3 P G(P,T)U(N) + \eta_1 P\left(d_1 + \frac{s_1}{H}\right) + \eta_2 T\left(d_2 + \frac{s_2}{H}\right).
\end{aligned}
\tag{1}
$$

N is assumed to be a limiting nutrient for P, but not for T. The nutrient is supplied by both mixing and from external sources (e.g., terrestrial run-off and/or turbulent diffusion), as well as from recycling of both P and T, and the total concentration of nutrient entering the water column has constant concentration N^0 and is entering the water column at the rate $\frac{D}{H}$, which is inversely proportional to the maximal mixing depth H (see Diehl 2002). In the absence of P and T, the concentration of N would approach N^0.

The specific loss rates of P and T are assumed to occur from death and sinking, as well as from water leaving the water column at the same rate that it is entering. The death rate of P is denoted by d_1 and of T by d_2. These rates are assumed to be independent of the column depth. Sinking is assumed to be proportional to sinking velocity, denoted by s_1 for P and s_2 for T. It is assumed that both the sinking and washout loss are inversely proportional to H, as described in Diehl (2002). N is recovered due to recycling of the P and T that dies or sinks at recycling rate η_1 for P and η_2 for T. It is assumed that $0 \le \eta_i < 1$, $i = 1, 2$, since only a fraction of the biomass that is recycled becomes nutrient N.

The maximum growth rate of P is denoted by μ_1 and of T by μ_2, and μ_3 denotes the maximal uptake rate. The function $U(N)$ is proportional to the uptake rate of nutrient N by P when limitation by light is ignored. It is reasonable to assume that the function $U(N)$ is continuously differentiable (C^1) and satisfies:

$$
U(0) = 0, \ U'(N) > 0, \ \lim_{N \to \infty} U(N) = 1.
$$

The function $G(P, T)$ models the effect of the light intensity on the growth of both P and T. For a discussion of several different approaches to modelling $G(P, T)$ see Grover (1997). Although one might assume that light and nutrient are essential nutrients and model their effect on growth using Liebig's Law of the minimum, Huisman and Weissing (1994, 1995) who have used that approach, provide a justification for using a different approach that we think is more realistic. This alternative approach was also used in Boushaba and Pascual (2005) and is used here. Instead, light and nutrient are assumed to be interactive essential nutrients for the growth of P, and although in the total absence of either there is no growth, the growth of P depends

on the limiting nutrient level enhanced by a factor representing the photosynthetic response to available light resulting in a multiplicative terms.

As described in Stomp et al. (2004), the vertical light gradient depends mainly on the incident light intensity (I_{in}) at the water surface, the light spectrum, and the light absorption by the phytoplankton species and suspended nutrient. According to Lambert-Beer's law, light intensity is constant at the water surface and declines exponentially with depth, so that the underwater vertical light gradient, as a function of the depth from the surface, h, can be described as,

$$I(P, T; \lambda, h) = I_{in}(\lambda) \exp((-k_{bg}(\lambda) - k_1(\lambda)P - k_2(\lambda)T)h), \qquad (2)$$

where λ denotes the wave length (assumed here to be constant), $k_{bg}(\lambda)$ the light attenuation coefficient of background turbidity caused by all non-phytoplankton components, and $k_i(\lambda)$, $(i = 1, 2)$ the specific light attenuation coefficient of P and T, respectively.

Following the approach in Boushaba and Pascual (2005), Diehl (2002), we average the local light over a mixed layer of depth H. Then I is approximated by a function, $G(P, T; \lambda, H)$ related to the maximum depth H, instead of the water depth h. For simplicity, we denote $G(P, T) := G(P, T; \lambda, H)$, since both λ and H are constants.

We re-scale model (1) by making the change of variables $\widehat{P} = \frac{\mu_3}{\mu_1} P$, defining $G(\widehat{P}, T) = G(\frac{\mu_1}{\mu_3}\widehat{P}, T) = G(P, T)$, and then dropping the hats for convenience. We then also define

$$D_H = \frac{D}{H}, \quad s_i^H = \frac{s_i}{H}, \ (i = 1, 2)$$
$$m_i = D_H + d_i + s_i^H \ (i = 1, 2),$$
$$\xi_1 = \frac{\mu_1 \eta_1 (d_1 + s_1^H)}{\mu_3 (D_H + d_1 + s_1^H)}, \xi_2 = \frac{\eta_2 (d_2 + s_2^H)}{D_H + d_2 + s_2^H}. \qquad (3)$$

Under this change of variables system (1) can be rewritten as:

$$P' = \mu_1 P G(P, T) U(N) - m_1 P \qquad (4a)$$
$$T' = \mu_2 T G(P, T) - m_2 T \qquad (4b)$$
$$N' = D_H(N^0 - N) - \mu_1 P G(P, T) U(N) + \xi_1 m_1 P + \xi_2 m_2 T. \qquad (4c)$$

By definition, $m_i > D_H$, $i = 1, 2$, and $0 \le \xi_2 < 1$, since $0 \le \eta_2 < 1$. We assume also that $0 \le \xi_1 < 1$. This follows for example, if $\mu_3 \ge \mu_1$ or if $\mu_1 > \mu_3$, is not too much bigger than μ_3. The former case is more likely, since more than one unit of nutrient usually needs to be consumed by P to produce one unit of P.

In the remainder of the manuscript, unless otherwise stated, we consider the rescaled model (4a, 4b, 4c), assuming that the functions $G(P, T)$ and $U(N)$ are C^1 and satisfy the following:

A(i) $G(0, 0) > 0$, $\frac{\partial G}{\partial P} < 0$, $\frac{\partial G}{\partial T} < 0$, $\lim_{P \to \infty} G(P, 0) = 0$, $\lim_{T \to \infty} G(0, T) = 0$,

A(ii) $U(0) = 0$, $U'(N) > 0$, $\lim_{N \to \infty} U(N) = 1$.

Examples of functions that satisfy assumptions **A(ii)** include: $U(N) = \dfrac{N^p}{N^p + \delta^p}$, where p and δ are all positive constants. Functions of the form $G(P, T) = \dfrac{\theta}{P^q + T^q + k}$ where θ and k are all positive constants, and $q \geq 1$ satisfy **A(i)**. If the effect of light is modelled differently, by using a Holling type II function $\dfrac{\hat{I}}{I_s + \hat{I}}$, where I_s denotes the half-saturation constant for light-limited growth, and $\hat{I}$ is given in (2), then the light averaged in a mixed layer can be described by

$$G(P, T) = \frac{1}{H} \int_0^H \frac{\hat{I}}{I_s + \hat{I}} dh = \frac{\ln(I_s + I_{in}) - \ln(I_s + I_{out})}{(k_{bg} + k_1 P + k_2 T) H}, \qquad (5)$$

where H is as before, and $I_{out} = I_{in} \exp([-k_{bg} - k_1 P - k_2 T] H)$. The proof that this function G satisfies **A(i)** is provided in Appendix B.

Boushaba and Pascual (2005) consider the special case

$$U(N) = \frac{N}{K + N} \quad \text{and} \quad G(P, T) = \frac{\epsilon I_0}{H[k_x + k_P(P + T)]}. \qquad (6)$$

i.e., they assume a Holling type II response function $U(N)$ with half saturation constant K, they replaced a factor $(1 - exp(-[kx + kP(P + T)]H))$ that appears in their derivation of G by the constant ϵ and I_0 denotes the irradiance intensity at the surface of the water, k_P denotes the phytoplankton-specific attenuation coefficient, and k_x is the short-wave extinction.

All of these forms satisfy our general assumptions **A(i)–(ii)**. Instead of using specific forms for the functions G and U in our theoretical results, we consider more general forms satisfying only A(i) and A(ii). This will help us determine how the form of these functions influence the dynamics. Using this approach, the analysis is more involved. However, the results apply more generally and our conclusions can be adopted more directly by other researchers. As well, we interpret the biologically relevant parameters S_P and S_T in the model of Boushaba and Pascual (2005).

3 Qualitative analysis of system (4a, 4b, 4c)

3.1 Well-posedness and competition independent extinction

We begin the analysis by showing that system (4a, 4b, 4c) is well-posed, i.e. solutions are uniformly bounded and non-negative. Since the vector field is C^1, uniqueness of solution to initial value problems holds. However, it is particularly interesting to note that unlike for most chemostat models, $N(t)$ is not necessarily asymptotically bounded above by $N^0 + \epsilon$, for arbitrary $\epsilon > 0$.

Theorem 1 *Consider the solutions of* (4a, 4b, 4c) *for which* $P(0) \geq 0$, $T(t) \geq 0$, *and* $N(0) \geq 0$.

1. *If $N(0) \geq 0$, then $N(t) > 0$ for all $t > 0$.*
   If $P(0) = 0$, then $P(t) = 0$ for all $t \geq 0$. If $P(0) > 0$, then $P(t) > 0$ for all $t \geq 0$.
   If $T(0) = 0$, then $T(t) = 0$ for all $t \geq 0$. If $T(0) > 0$, then $T(t) > 0$ for all $t \geq 0$.
2. *Select any $\epsilon > 0$, $\overline{P} > 0$ and $\overline{T} > 0$ such that $G(\overline{P}, 0) < \frac{m_1}{\mu_1}$, $G(0, \overline{T}) < \frac{m_2}{\mu_2}$. Then the set*

$$\mathcal{K} = \left\{ (P, T, N) : 0 \leq P \leq \overline{P}, \ 0 \leq T \leq \overline{T}, \ 0 \leq N \leq N^0 + \frac{\xi_1 m_1 \overline{P} + m_2 \xi_2 \overline{T}}{D_H} + \epsilon \right\}.$$

   is a positively invariant compact attracting set, and hence the system is point dissipative.
3. *If $G(0, 0) < \frac{m_1}{\mu_1}$, then $P \to 0$ as $t \to \infty$; If $G(0, 0) < \frac{m_2}{\mu_2}$, then $T \to 0$ as $t \to \infty$.*

Proof 1. The results are straightforward since $\dot{N}|_{N=0} > 0$, the plane with $N = 0$ repels into the interior of the positive cone, each coordinate plane where either $P = 0$ or $T = 0$ is invariant in the vector field C^1, and all the solutions cannot reach the boundary of the positive cone in finite time by the uniqueness of solutions of initial value problems.

2. Note that by assumption **A(i)**, such $\overline{P} > 0$ and $\overline{T} > 0$ always exist. Select any solution with $(P(0), T(0), N(0))$ in the positive cone. First we show that there exists a time $t_1 \geq 0$ such that $T(t_1) < \overline{T}$. Otherwise, if $T(t) \geq \overline{T}$ for all $t > 0$, then $T'(t) \leq T(t)(\mu_2 G(0, \overline{T}) - m_2)$, and since $\mu_2 G(0, \overline{T}) - m_2 < 0$, it would follow that $T'(t) \to 0$ as $t \to \infty$, a contradiction. Now if for some $t \geq t_1$, $T(t_1) = \overline{T}$, then $T'(t) < 0$. Hence, $T(t) \leq \overline{T}$ for all $t > t_1$. Since $U(N) < 1$ for all $N \geq 0$, $P'(t) \leq P(t)(\mu_1 G(P(t), T(t)) - m_1)$, for all $t \geq 0$. It now follows similarly that there exists $t_2 \geq 0$ such that $P(t) \leq \overline{P}$ for all $t \geq t_2$. It then follows that for all $t \geq t_3 = \max\{t_1, t_2\}$, $N'(t) \leq D_H(N^0 - N(t)) + \xi_1 m_1 \overline{P} + \xi_2 m_2 \overline{T}$. If $N(t) \geq N^0 + \frac{\xi_1 m_1 \overline{P} + m_2 \xi_2 \overline{T}}{D_H} + \epsilon$ for all $t \geq t_3$, then $N'(t) \leq -\epsilon D_H < 0$, which implies that $N(t) \to -\infty$ as $t \to \infty$, a contradiction. Hence, there exists $t_4 \geq t_3$ such that $N(t) \leq N^0 + \frac{\xi_1 m_1 \overline{P} + m_2 \xi_2 \overline{T}}{D_H} + \epsilon$ for all $t \geq t_4$. In part *1.* we showed that all components remain nonnegative. Hence, the result follows.

3. The results follow immediately from Eqs. (4a) and (4b), and assumption **A(i)**.
□

Next we state results concerning competition-independent extinction.

Theorem 2 *Consider system* (4a, 4b, 4c).

1. *If $G(0, 0) < \frac{m_1}{\mu_1}$, then $P \to 0$ as $t \to \infty$.*
2. *If $G(0, 0) < \frac{m_2}{\mu_2}$, then $T \to 0$ as $t \to \infty$.*

Proof These results follow immediately from Eqs. (4a) and (4b), and assumption **A(i)**.
□

3.2 Existence of steady-state solutions of system ([4a](#), [4b](#), [4c](#))

We denote the "washout" equilibrium where neither phytoplankton is present and the nutrient remains at the concentration N^0 by $E_0 = (0, 0, N^0)$. Equilibria of the following form (where the components not indicated explicitly by zero are assumed to be positive) are also possible for system ([4a](#), [4b](#), [4c](#)):

$$E_1 = \left(P_1^*, 0, N_1^*\right), \quad E_2 = \left(0, T_2^*, N_2^*\right), \quad E_3 = \left(P^*, T^*, N^*\right).$$

In this subsection we determine under what conditions these equilibrium points exist.

First we consider the existence of a single species survival steady-state of the form E_1 for which only the non-nitrogen-fixing population survives.

Theorem 3 *There is a single species survival steady-state of the form $E_1 = \left(P_1^*, 0, N_1^*\right)$, if and only if*

$$G(0, 0) > \frac{m_1}{\mu_1 U(N^0)}. \tag{7}$$

If ([7](#)) holds, then

$$P_1^* = \frac{D_H}{m_1(1 - \xi_1)}(N^0 - N_1^*), \tag{8}$$

where $N_1^* < N^0$ is the unique solution of

$$G\left(\frac{D_H}{m_1(1 - \xi_1)}(N^0 - N_1^*), 0\right) = \frac{m_1}{\mu_1 U(N_1^*)}. \tag{9}$$

Proof By Eq. ([4a](#)), P_1^* and N_1^* must satisfy

$$\mu_1 G(P_1^*, 0)U(N_1^*) = m_1. \tag{10}$$

Substituting this in Eq. ([4c](#)) and solving for P_1^*, it follows that if a solution N_1^* exists, then P_1^* must satisfy ([8](#)), and since $P_1^* > 0$, then $N_1^* < N^0$. By **A(i)–(ii)**, G is a decreasing function of P and U is an increasing function of N. Hence, ([10](#)) can only be satisfied if ([7](#)) holds, hence ([7](#)) is a necessary condition. Now, replacing P in ([4c](#)) by P_1^* in ([8](#)), it follows that N_1^* must satisfy ([9](#)).

It remains to show that a solution $0 < N_1^* < N^0$ of ([9](#)) exists and that it is unique. Define

$$l(N) := G\left(\frac{D_H}{m_1(1 - \xi_1)}(N^0 - N), 0\right) \quad \text{and} \quad r(N) := \frac{m_1}{\mu_1 U(N)}.$$

We show that there is a unique solution satisfying $l(N_1^*) = r(N_1^*)$, $0 < N_1^* < N^0$, provided that ([7](#)) holds. $l(0) < \lim_{N \to 0} r(N) = \infty$, and by ([7](#)), $l(N^0) = G(0, 0) > \frac{m_1}{\mu_1 U(N^0)} = r(N^0)$. By **A(ii)**, $l'(N) > 0$ and $r'(N) < 0$ for $N \in (0, N^0)$. Therefore, there is a unique intersection point, $N_1^* \in (0, N^0)$, and the result follows. $\qquad \square$

Next we consider the existence of a single species survival steady-state of the form E_2 for which only the nitrogen-fixing population survives.

Theorem 4 *There is a single species steady-state of the form E_2 if and only if*

$$G(0, 0) > \frac{m_2}{\mu_2}. \tag{11}$$

When (11) holds, T_2^* is uniquely defined by

$$G(0, T_2^*) = \frac{m_2}{\mu_2} \tag{12}$$

and

$$N_2^* = N^0 + \frac{\xi_2 m_2 T_2^*}{D_H} \geq N^0. \tag{13}$$

Hence, there is at most one steady-state of the form E_2.

Proof From Eq. (4b), T_2^* must satisfy: $G(0, T_2^*) = \frac{m_2}{\mu_2}$. By (**A(i)**), $G(0, 0) > G(0, T_2^*)$, since G is decreasing with respect to T. Therefore, $T_2^* > 0$ exists if and only if (11) holds, and T_2^* is uniquely defined by (12). That $N_2^* = N^0 + \frac{\xi_2 m_2 T_2^*}{D_H} \geq N^0$ follows by substituting T_2^* in the RHS of Eq. (4c), setting this equal to 0, and solving for N_2^*. □

It is worth emphasizing here that when $\xi_2 > 0$, then $N_2^* > N^0$. This occurs due to the production of nitrogen by the nitrogen-fixing Trichodesmium. This differs from the phytoplankton-nutrient models or chemostat models with nutrient recycling in the literature, that do not include a nitrogen-fixing population (Edwards and Brindley 1997).

Finally, we consider when a coexistence steady-state of the form E_3 for which both the non-nitrogen-fixing and the nitrogen-fixing populations survive exists.

For convenience of notation, define

$$\xi = \frac{m_1 \mu_2}{m_2 \mu_1}.$$

Theorem 5 *There is a unique coexistence equilibrium of the form E_3 if and only if*

$$\xi < 1, \tag{14}$$

$$G(0, 0) > \frac{m_1}{\mu_1}, \tag{15}$$

and one of the following holds:

1. $U^{-1}(\xi) < N^0$ *and* $G(\frac{D_H(N^0 - U^{-1}(\xi))}{m_1(1 - \xi_1)}, 0) > \frac{m_2}{\mu_2}$, *or*
2. $\xi_2 > 0$, $U^{-1}(\xi) \geq N^0$, *and* $G\left(0, \frac{D_H(U^{-1}(\xi) - N^0)}{m_2 \xi_2}\right) > \frac{m_2}{\mu_2}$.

In both cases

$$N^* = U^{-1}(\xi), \tag{16}$$

In Case 1, define the function $P(T) := \frac{D_H(N^0 - U^{-1}(\xi)) + \xi_2 m_2 T}{m_1(1 - \xi_1)}$. Then T^* is the unique solution of $G(P(T), T) = \frac{m_2}{\mu_2}$ and $P^* = P(T^*)$.

In Case 2, define the function $T(P) := \frac{D_H(U^{-1}(\xi) - N^0)) + m_1(1 - \xi_1)P}{m_2 \xi_2}$. Then P^* is the unique solution of $G(P, T(P)) = \frac{m_2}{\mu_2}$ and $T^* = T(P^*)$.

Proof At the steady-state E_3, by Eq. (4b),

$$G(P^*, T^*) = \frac{m_2}{\mu_2}, \tag{17}$$

and by Eq. (4a),

$$G(P^*, T^*) = \frac{m_1}{\mu_1 U(N^*)}. \tag{18}$$

Therefore, by **A(i)–(ii)**, it follows that P^* and T^* can only be found, if (15) holds. Equating the right hand sides of (17) and (18), it follows that N^* is uniquely defined by (16) provided (14) holds.

Case 1. Substituting (16) and (17) in (4c) and solving for P^* as a function of T^*, it follows that

$$P^* = \frac{D_H(N^0 - U^{-1}(\xi)) + \xi_2 m_2 T^*}{m_1(1 - \xi_1)} = P(T^*).$$

$P(T)$ is an increasing function of T. Define $F_1(T) := G(P(T), T)$, which is a decreasing function of T with $\lim_{T \to \infty} F_1(T) = 0$ by **A(i)**. But then (17) becomes $F_1(T^*) = \frac{m_2}{\mu_2}$, and hence a unique solution always exists provided that $F_1(0) = G(P(0), 0) = G(\frac{D_H(N^0 - U^{-1}(\xi))}{m_1(1 - \xi_1)}, 0) > \frac{m_2}{\mu_2}$.

Case 2. If $\xi_2 > 0$ and $U^{-1}(\xi) > N^0$, substituting (16) and (17) in (4c) and solving for T^* as a function of P^*, if $\xi_2 > 0$, it follows that

$$T^* = \frac{D_H(U^{-1}(\xi) - N^0)) + m_1(1 - \xi_1)P^*}{m_2 \xi_2} = T(P^*).$$

The argument is now similar to the argument for Case 1. Define $F_2(P) := G(P, T(P))$, which is then a decreasing function of P and by **A(i)**, $\lim_{P \to \infty} F_2(P) = 0$. But then (17) implies that $F_2(P^*) = \frac{m_2}{\mu_2}$. Hence a unique solution always exists provided that $F_2(0) = G(0, T(0)) = G\left(0, \frac{D_H(U^{-1}(\xi) - N^0)}{m_2 \xi_2}\right) > \frac{m_2}{\mu_2}$. On the other hand, in this case $\xi_2 > 0$ is necessary for E_3 to exist, since if $\xi_2 = 0$, by substituting (16) and (17) in (4c), it follows that $P^* \leq 0$.   □

Again it is noteworthy that the concentration of nitrogen at the coexistence steady-state is always less than N^0 if $\xi_2 = 0$, but if $\xi_2 > 0$ it can be less than N^0, equal to N^0, or greater than N^0. This depends upon the productivity level of the nitrogen-fixing population, T.

We conclude this subsection by pointing out that there is no coexistence steady-state E_3 unless the single species equilibrium point E_2 also exists.

Theorem 6 *If E_3 exists, then E_2 also exists.*

Proof In order for E_3 to exist, one of the conditions 1. or 2. in Theorem 5 must hold. By **A(i)**, $G(P, T)$ is a decreasing function of both P and T, and so $G(0, 0) > \frac{m_2}{\mu_2}$ must hold. By Theorem 4, it follows immediately that E_2 also exist. □

3.3 Local stability of equilibria of system (4a, 4b, 4c)

Here we give conditions for the local stability of the steady-states. The proofs not shown can be found in Appendix A.

Theorem 7 1. *E_0 is locally asymptotically if $G(0, 0) < \min \left\{ \frac{m_1}{\mu_1 U(N^0)}, \frac{m_2}{\mu_2} \right\}$, and unstable if the inequality is reversed.*
2. *When E_1 exists, i.e. (7) is satisfied, then it is locally asymptotically stable if, $G(P_1^*, 0) < \frac{m_2}{\mu_2}$, or equivalently $U(N_1^*) > \xi$, and unstable if these inequalities are reversed.*
3. *When E_2 exists, i.e. (11) is satisfied, then it is locally asymptotically stable if, $G(0, T_2^*) < \frac{m_1}{\mu_1 U(N_2^*)}$ or equivalently, $U(N_2^*) < \xi$, and is unstable if these inequalities are reversed.*

Corollary 8 *If both E_1 and E_2 exist, at most one of them is locally asymptotically stable.*

Proof By Theorems 3 and 4 a necessary condition for both E_1 and E_2 to exist is that $G(0, 0) > \max \left\{ \frac{m_1}{\mu_1 U(N^0)}, \frac{m_2}{\mu_2} \right\}$. By Theorem 7, for E_1 to be locally asymptotically stable, $\frac{m_1}{\mu_1 U(N_1^*)} = G(P_1^*, 0) < \frac{m_2}{\mu_2}$, whereas for E_2 to be locally asymptotically stable $\frac{m_2}{\mu_2} = G(0, T_2^*) < \frac{m_1}{\mu_1 U(N_2^*)}$. But since $N_1^* < N^0 \leq N_2^*$, both these conditions cannot be satisfied at the same time. □

Theorem 9 *If E_3 exists, then E_3 is locally asymptotically stable if the right hand side of (27) in Appendix A is positive and unstable if it is negative. In particular, if*

$$\xi_2 = 0 \quad or \quad (m_1 - m_2)(1 - \xi_1) + D_H \geq 0, \tag{19}$$

then E_3 is locally asymptotically stable.

Note that (19) is only a sufficient condition for the local asymptotic stability of E_3. All of our numerical investigations seem to indicate that, in fact, E_3 is globally asymptotically stable when it is locally asymptotically stable. However, in Sect. 4 using numerical continuation of bifurcation curves we show that it can lose stability undergoing a Hopf bifurcation. In Sect. 3.5 we are able to prove that when E_3 exists, all populations are uniformly persistent using the following result that implies that when E_3 exists all other steady-states are unstable.

Theorem 10 *E_3 exists if and only if* (i) *E_0 exists and is unstable,* (ii) *E_2 exists and is unstable, and* (iii) *either E_1 does not exist or E_1 exists and is unstable.*

Proof E_0 always exists. If E_3 exists, by Theorem 6, E_2 exists, and so by Theorem 4, $G(0,0) > \frac{m_2}{\mu_2}$. Hence, by Theorem 7, E_0 is unstable. To show that E_2 is unstable, it suffices to show that $\frac{m_1}{\mu_1 U(N_2^*)} < \frac{m_2}{\mu_2}$, since by (12), $G(0, T_2^*) = \frac{m_2}{\mu_2}$. If $\xi_2 = 0$, only case 1 of Theorem 5 can be satisfied. In this case $N^* = U^{-1}(\xi) < N^0 = N_2^*$, by Theorem 4. Therefore, $\frac{m_1}{\mu_1 U(N_2^*)} = \frac{m_1}{\mu_1 U(N^0)} < \frac{m_1}{\mu_1 U(N^*)} = G(P^*, T^*) = \frac{m_2}{\mu_2}$, and so E_2 is unstable. If $\xi_2 > 0$ by (13), it follows that $T_2^* = \frac{D_H(N_2^*-N^0)}{m_2 \xi_2}$. In case 1 of Theorem 5, since $N^* \leq N^0 < N_2^*, U(N_2^*)U(N^*) = \xi$, and so $\frac{m_1}{\mu_1 U(N_2^*)} < \frac{m_2}{\mu_2}$. Hence, E_2 is unstable. In case 2, $N^* > N^0$, and either $N^* \leq N_2^*$ and the argument is the same as in case 1, or $N^* > N_2^*$. But $N^* > N_2^*$ is impossible, since if $N^* > N_2^*$, due to the fact that $G(0, T)$ is decreasing in T, $\frac{m_2}{\mu_2} = G(0, T_2^*) = G\left(0, \frac{D_H(N_2^*-N^0)}{m_2 \xi_2}\right) > G\left(0, \frac{D_H(N^*-N^0)}{m_2 \xi_2}\right) > \frac{m_1}{\mu_1 U(N^*)} = \frac{m_2}{\mu_2}$, a contradiction. When E_3 exists, (7) does not necessarily hold, i.e., E_1 may not exist.

Next consider the stability of E_1 when E_3 and E_1 exist. In case 1 of Theorem 5, if $N^* > N_1^*$, since $G(P_1^*, 0) = \frac{m_1}{\mu_1 U(N_1^*)} > \frac{m_1}{\mu_1 U(N^*)} = \frac{m_2}{\mu_2}$, and so by Theorem 7, E_1 is unstable. If on the other hand, $N^* \leq N_1^*, G(P_1^*, 0) = G\left(\frac{D_H(N^0-N_1^*)}{m_1(1-\xi_1)}, 0\right) \geq G\left(\frac{D_H(N^0-N^*)}{m_1(1-\xi_1)}, 0\right) > \frac{m_1}{\mu_1 U(N^*)} = \frac{m_1}{\mu_1 \xi} = \frac{m_2}{\mu_2}$, and so again by Theorem 7, E_1 is unstable. In case 2, $N_1^* < N^0 < N^*$. The argument is the same as in case 1 when $N^* > N_1^*$, and again E_1 is unstable.

Next we show that if (ii) and (iii) hold, then E_3 exists. If (ii) holds, by Theorem 7 $\xi < U(N_2^*)$. By **A(ii)**, $U(N_2^*) < 1$. Hence, $\xi < 1$. Also, $\frac{m_1}{\mu_1} < \frac{m_2 U(N_2^*)}{\mu_2} < G(0, T_2^*) < G(0, 0)$, and hence $G(0, 0) > \frac{m_1}{\mu_1}$. If (iii) holds as well, when E_1 exists and is unstable, then by Theorem 7 $U(N_1^*) < \xi$, i.e., $N_1^* < U^{-1}(\xi)$. Therefore, if $U^{-1}(\xi) \leq N^0$, then $G\left(\frac{D_H(N^0-U^{-1}(\xi))}{m_1(1-\xi_1)}, 0\right) > \frac{m_2}{\mu_2}$. If instead, $\xi_2 > 0$ and $U^{-1}(\xi) > N^0$, then since E_2 is unstable $U(N^0) < \xi < U(N_2^*)$, and so $G\left(0, \frac{D_H(U^{-1}(\xi)-N^0)}{m_2 \xi_2}\right) > G(0, T_2^*) = \frac{m_2}{\mu_2}$, Therefore, E_3 exists. When instead E_1 does not exist and E_2 is unstable, $\frac{m_2}{\mu_2} < G(0, 0) \leq \frac{m_1}{\mu_1 U(N^0)}$, and hence $U(N^0) < \xi$ and so $N^0 < U^{-1}(\xi) < N_2^*$. Then, $G\left(0, \frac{D_H(U^{-1}(\xi)-N^0)}{m_2 \xi_2}\right) > G(0, T_2^*) = \frac{m_2}{\mu_2}$. Therefore, E_3 exists. $\square$

3.4 Global stability of equilibria of system (4a, 4b, 4c)

The relevance of local stability for ecosystem dynamics has been questioned, since it might be possible to have more than one attracting state with the outcome dependent on the initial state of the system. For this reason whenever possible it is important to determine conditions that guarantee global stability of an attracting state, and when this is not possible, to at least find conditions that predict that all of the populations survive.

First we consider the global dynamics when at least one population is absent, i.e., either $P(0) = 0$ or $T(0) = 0$.

Theorem 11   1. *Assume that $T(0) = 0$. Then, $T(t) = 0$ for all $t \geq 0$, and*
   (a) *if $G(0,0) \leq \frac{m_1}{\mu_1 U(N^0)}$, then $\lim_{t \to \infty} P(t) = 0$ and $\lim_{t \to \infty} N(t) = N^0$;*
   (b) *if $P(0) > 0$ and $G(0,0) > \frac{m_1}{\mu_1 U(N^0)}$, then $\lim_{t \to \infty} P(t) = P_1^* > 0$, and $\lim_{t \to \infty} N(t) = N_1^* < N^0$, where P_1^* and N_1^* were defined by* (8) *and* (9), *respectively.*
2. *Assume that $P(0) = 0$. Then, $P(t) = 0$ for all $t \geq 0$, and*
   (a) *if $G(0,0) \leq \frac{m_2}{\mu_2}$, then $\lim_{t \to \infty} T(t) = 0$ and $\lim_{t \to \infty} N(t) = N^0$;*
   (b) *if $T(0) > 0$ and $G(0,0) > \frac{m_2}{\mu_2}$, then $\lim_{t \to \infty} T(t) = T_2^* > 0$, and $\lim_{t \to \infty} N(t) = N_2^* \geq N^0$, where T_2^* and N_2^* were defined by* (12) *and* (13), *respectively and equality holds when $\xi_2 = 0$.*

Proof The plane where $T = 0$ is clearly invariant. Restricted to the $(P, 0, N)$ plane, system (4a, 4b, 4c) satisfies the reduced system:

$$P' = \mu_1 P G(P, 0) U(N) - m_1 P \tag{20a}$$
$$N' = D_H(N^0 - N) - \mu_1 P G(P, 0) U(N) + \xi_1 m_1 P. \tag{20b}$$

By Theorem 3, in case 1(a), E_0 is the only steady-state solution, and in case 1(b) E_0 and E_1 are the only steady-state solutions. Solutions are bounded by Theorem 1. Therefore, in case 1(a), that E_0 is globally asymptotically stable follows by the Poincaré-Bendixson Theorem.

In case 1(b) from the local analysis in Appendix A, E_0 is unstable, and restricted to the $(P, 0, N)$ plane, E_1 is locally asymptotically stable. Applying the Dulac Criterion in the region $\mathcal{D}_P = \{(P, 0, N) : P > 0, N > 0\}$ with auxiliary function $\beta(P, T) = \frac{1}{P}$, since

$$\frac{\partial}{\partial P}(\beta P') + \frac{\partial}{\partial N}(\beta N') = \mu_1 \frac{\partial}{\partial P} G(P, 0) U(N) - \frac{D_H}{P} - \mu_1 G(P, 0) U'(N) < 0,$$

there are no nontrivial periodic orbits in the region $\mathcal{D}_P$. Since solutions are bounded, applying the Poincaré-Bendixson Theorem, it follows that in this case E_1 is globally asymptotically stable with respect to solutions initiating in $\mathcal{D}_P$.

Next consider case 2. The plane where $P = 0$ is clearly invariant. Restricted to the $(0, T, N)$ plane, system (4a, 4b, 4c) satisfies the reduced system:

$$T' = \mu_2 T G(0, T) - m_2 T \tag{21a}$$
$$N' = D_H(N^0 - N) + \xi_2 m_2 T. \tag{21b}$$

In case 2(a), that E_0 is globally asymptotically stable follows by a similar argument using Theorem 4 instead.

In case 2(b) from the local analysis in Appendix A, E_0 is unstable, and restricted to the $(0, T, N)$ plane, E_1 is locally asymptotically stable. Applying the Dulac Criterion in the region $\mathcal{D}_T = \{(0, T, N) : T > 0, N > 0\}$ with auxiliary function $\beta(P, T) = \frac{1}{T}$, since

$$\frac{\partial}{\partial T}(\beta T') + \frac{\partial}{\partial N}(\beta N') = \mu_2 \frac{\partial}{\partial T}G(0, T) - \frac{D_H}{T} < 0,$$

there are no nontrivial periodic orbits in the region $\mathcal{D}_T$. In this case, that E_2 is globally asymptotically stable with respect to solutions initiating in $\mathcal{D}_T$ is similar to that given for case 1(b). □

We can now extend some of the local stability results given in Theorem 7 to global stability.

Theorem 12 *Consider system* (4a, 4b, 4c) *with initial conditions in the set* $\mathcal{C} = \{(P, T, N) : P > 0, \ T > 0, \ N \geq 0\}$.

1. *If* $G(0, 0) \leq \min\left\{\dfrac{m_1}{\mu_1 U(N^0)}, \dfrac{m_2}{\mu_2}\right\}$, *then* E_0 *is globally asymptotically stable;*
2. *If* $\dfrac{m_1}{\mu_1 U(N^0)} < G(0, 0) \leq \dfrac{m_2}{\mu_2}$, *then* E_1 *is globally asymptotically stable with respect to* $\mathcal{C}$;
3. *If* $\dfrac{m_2}{\mu_2} < G(0, 0) \leq \dfrac{m_1}{\mu_1}$, *then* E_2 *is globally asymptotically stable with respect to* $\mathcal{C}$.

Proof First assume, as in cases 1 and 2, that $G(0, 0) \leq \frac{m_2}{\mu_2}$. We show that $T(t) \to 0$ as $t \to \infty$. Since $P(0) > 0$ and $T(0) > 0$, by Theorem 1, $P(t) > 0$ and $T(t) > 0$ for all $t > 0$, and so by **A(i)**, $G(P(t), T(t)) < G(P(t), 0) < G(0, 0) \leq \frac{m_2}{\mu_2}$ for all $t > 0$. Therefore, $T'(t) < (\mu_2 G(P(t), 0) - m_2)T(t) \leq 0$, and since $T(t)$ is bounded below by 0, $T(t) \to L \geq 0$, finite, as $t \to 0$. If $L > 0$, then $T(t) > L/2$ for all sufficiently large t, and so $T'(t) = (\mu_2 G(P(t), T(t)) - m_2)T(t) < (\mu_2 G(0, \frac{L}{2}) - m_2)T(t) = \alpha T(t)$, where $\alpha = \mu_2 G(0, \frac{L}{2}) - m_2 < 0$. Therefore, $T(t) \to 0$ as $t \to \infty$, in both cases 1 and 2.

In case 1, by Theorems 3 and 4, E_0 is the only steady-state solution of (4a, 4b, 4c). Since $T(t) \to 0$ as $t \to \infty$, first consider the limiting system (20a, 20b), i.e., the system with initial conditions restricted to the $(P, 0, N)$ plane. It follows that the only equilibrium point in the (P, N) plane is $(0, N^0)$, and by Theorem 11(1a), it is globally asymptotically stable in this plane. To show that $E_0 = (0, 0, N^0)$ is globally asymptotically stable for the full system (4a, 4b, 4c), let $r(t) = (P(t), T(t), N(t))$ be an arbitrary solution with $P(0) \geq 0, T(0) \geq 0, N(0) \geq 0$. Since we showed that $T(t) \to 0$ as $t \to \infty$, any point in the omega-limit set of $r(t)$, denoted by $\omega(r)$, must be of the form $W = (P, 0, N)$ with $P \geq 0$ and $N \geq 0$. Due to the invariance of $\omega(r)$, the entire orbit through W must be in $\omega(r)$. Since E_0 is globally asymptotically stable with respect to the solutions starting on the coordinate plane $T = 0$ and $\omega(r)$ is closed, E_0 must be in $\omega(r)$. Since E_0 is locally asymptotically stable for the full system (4a, 4b, 4c), it must be the only point in $\omega(r)$. The result in case 1 follows.

Next consider case 2. In this case there are two steady state solutions for (4a, 4b, 4c), E_0 and E_1. E_1 is locally asymptotically stable and E_0 is unstable. From the calculations in Appendix A, E_0 has a 1-dimensional stable manifold restricted to the axis where $P = 0$ and $T = 0$. We have already shown that in this case, $T(t) \to 0$ as $t \to \infty$. We again first restrict attention to (20a, 20b), the limiting system in the (P, N) plane. The

steady-states E_0 and E_1 correspond to the steady state solutions $(0, N^0)$ and (P_1^*, N_1^*), respectively, in the (P, N) plane. For system (20a, 20b), $(0, N^0)$ is unstable with a 1-dimensional stable manifold restricted to the axis with $P = 0$, and by Theorem 11(1b), (P_1^*, N_1^*) is globally asymptotically stable in this plane with respect to solutions with $P(0) > 0$. Any point of the omega limit set of any solution of the full system (4a, 4b, 4c), initiating in $\mathcal{C}$ must be of the form $(P, 0, N)$. Since $(0, 0, N^0)$ is unstable with a 1-dimensional stable manifold restricted to the axis with $P = 0$, it cannot be the only point in the omega limit set, and so since $E_1 = (0, P_1^*, N_1^*)$ is globally asymptotically stable in the plane with respect to solutions with $T(0) = 0$ and $P(0) > 0$, E_1 must also be in the omega limit set. But since E_1 is locally asymptotically stable for (4a, 4b, 4c), E_1 must be the only point in the omega limit set, and hence E_1 is globally asymptotically stable for (4a, 4b, 4c) with respect to solutions starting in $\mathcal{C}$.

In case 3, if one notes that $U(N) < 1$ for all $N \geq 0$, then the result follows using similar arguments to those used in case 1, using the limiting system (21a, 21b) instead of (20a, 20b) and Theorem 11(2b) instead of Theorem 11(1b). □

3.5 Persistence of the populations

Obtaining conditions guaranteeing the long term survival i.e., persistence of populations, is a central issue in population biology. We address this issue in what follows.

Theorem 13 *System* (4a, 4b, 4c) *is uniformly persistent, in the sense that, there exists* $\delta > 0$ *such that if* $P(0) > 0$ *and* $T(0) > 0$, *then* $\liminf_{t \to \infty} P(t) > \delta$, *and* $\liminf_{t \to \infty} T(t) > \delta$, *provided that*

$$G(0, 0) > \frac{m_2}{\mu_2} \quad and \quad G(0, T_2^*) > \frac{m_1}{\mu_1 U(N_2^*)}, \tag{22}$$

and

$$either \ \left(G(0, 0) \leq \frac{m_1}{\mu_1 U(N^0)}\right) \ or \ \left(G(0, 0) > \frac{m_1}{\mu_1 U(N^0)} \ and \ G(P_1^*, 0) > \frac{m_2}{\mu_2}\right). \tag{23}$$

Proof By Theorems 4 and 7(3), the hypotheses in (22) imply that steady-state E_2 exists and is unstable. From the calculations in Appendix A and Theorem 11(2b), E_2 has a 2-dimensional stable manifold consisting of the portion of the $(0, T, N)$-plane with $T > 0$ and $N \geq 0$, and 1-dimensional unstable manifold repelling into the interior of $\mathbb{R}_+^3$. If the bracket on the left of (23) holds, then by Theorem 3, steady-state E_1 does not exist, and if the bracket on the right is satisfied, then E_1 exists, but by Theorem 7(2), is unstable. In the latter case, again from the calculations in Appendix A and Theorem 11(1b) E_1 has a 2-dimensional stable manifold consisting of the portion of the $(P, 0, N)$-plane with $P > 0$ and $N \geq 0$, and 1-dimensional unstable manifold repelling into the interior of $\mathbb{R}_+^3$. In both cases, E_0 is unstable. When E_1 does not exist, in the former case E_0 has a 2-dimensional stable manifold restricted to the $(P, 0, N)$ plane where $P \geq 0$ and $N \geq 0$, and in the latter case, a 1-dimensional stable manifold restricted to the N-axis. Since the dynamics on the boundary of $\mathbb{R}_+^3$

are completely understood by Theorem 11, using standard arguments applying the Butler-McGehee Lemma (see Freedman and Waltman 1984), it follows that the system is weakly persistent. However, weak persistence implies uniform persistence here (see Butler et al. 1986), since by Theorem 1, the system is point dissipative, and the boundary of $\mathbb{R}_+^3$ is isolated and acyclic.   □

Corollary 14 *Consider system* (4a, 4b, 4c). *The following are equivalent:*

1. E_3 *exists.*
2. E_0 *exists and is unstable,* E_2 *exists and is unstable, and either* E_1 *does not exist or* E_1 *exists and is unstable.*
3. *Both* (22) *and* (23) *hold.*
4. *System* (4a, 4b, 4c) *is uniformly persistent.*

Proof This is a direct consequence of Theorems 7, 10 and 13.

Alternatively, that the system is uniformly persistent implies that E_3 exists, since by Theorem 1, system (4a, 4b, 4c) is point dissipative, and so uniform persistence implies the existence of a steady-state with all components positive (see Hutson and Schmitt 1992; Zhao 2003).   □

3.6 Summary of the analytic results for system (4a, 4b, 4c)

Define,

$$e_1 = \frac{m_1}{\mu_1 U(N^0)}, \quad e_2 = \frac{m_2}{\mu_2}, \quad e_3 = \frac{m_1}{\mu_1}, \quad e_4 = \frac{m_1}{\mu_1 U(N_2^*)}, \quad e_5 = \frac{m_1}{\mu_1 U(N_1^*)},$$

where e_4 is only defined when E_2 exists and e_5 is only defined when E_1 exists. Then, $G(P_1^*, 0) = e_5$, $G(0, T_2^*) = e_2$, and since $N_1^* < N^0 \leq N_2^*$, it follows that $e_3 < e_4 \leq e_1 < e_5$. Note that all these inequalities are strict unless $\xi_2 = 0$. From the results in the previous subsections it follows that the number and stability of the steady-states depend on the relative values of the e_i and $G(0, 0)$. We summarize how the dynamics depends on these parameters in Table 1, keeping in mind that we have shown in Theorem 6 that E_3 does not exist unless E_2 also exists. Also, it follows from Theorem 7, Corollary 8, and Theorem 10 that at most one steady-state can be stable at a time, and by Corollary 14, that if E_3 exists the system is uniformly persistent.

4 Numerical exploration

In this section, first we explore the bifurcations exhibited by the model and the resulting change in dynamics when key parameters are varied. In particular, using numerical methods, we provide an example in which all of the cases in Table 1 occur for the appropriate selection of the parameters. We also demonstrate that competitor-mediated coexistence is possible.

Using the model studied by Boushaba and Pascual (2005), a special case of the model we analyzed in the previous sections, we demonstrate once more that all of the cases in Table 1 occur for appropriate choices of m_1 and m_2 using a two-parameter bifurcation diagram and using a one parameter bifurcation diagram that when

Table 1 Conditions for existence and stability of steady-states, and for uniform persistence of system (4a, 4b, 4c)

Case	Criterion	E_0	E_1	E_2	E_3	Dynamics
I	$G(0,0) < \min\{e_1, e_2\}$	l.a.s.	DNE	DNE	DNE	E_0 g.a.s.
II	$e_1 < G(0,0) \leq e_2$	u.s.	l.a.s.	DNE	DNE	E_1 g.a.s.
III	$e_2 < G(0,0) \leq e_1$ $e_2 < e_4$	u.s.	DNE	l.a.s.	DNE	E_2 g.a.s.[b] if $G(0,0) < e_3$
IV[d]	$e_2 < G(0,0) \leq e_1$ $e_2 > e_4$	u.s.	DNE	u.s.	l.a.s. if (27)[c] positive	Uniform persistence
V	$G(0,0) > \max\{e_1, e_2\}$ $e_2 < e_4$	u.s.	u.s.	l.a.s.	DNE	E_2 l.a.s.[b]
VI	$G(0,0) > \max\{e_1, e_2\}$ $e_2 > e_5$	u.s.	l.a.s.	u.s.	DNE	E_1 l.a.s.[a]
VII	$G(0,0) > \max\{e_1, e_2\}$ $e_5 > e_2 > e_4$	u.s.	u.s.	u.s.	l.a.s. if (27)[c] positive	Uniform persistence

We denote: does not exist, unstable, locally asymptotically stable, and globally asymptotically stable, by DNE, u.s., l.a.s., and g.a.s., respectively

[a] We conjecture that E_1 is g.a.s. whenever it is l.a.s.

[b] We conjecture that E_2 is g.a.s. whenever it is l.a.s. (e.g., even if $e_3 \geq G(0,0)$).

[c] Sufficient conditions for the local asymptotic stability of E_3 are $(m_2 - m_1)(1 - \xi_1) + D_H \geq 0$ or $\xi_2 = 0$.

[d] If $\xi_2 = 0$, then $N_2^* = N^0$ and so $e_1 = e_4$. Therefore, Case IV can only occur if $\xi_2 > 0$. If so, there is competitor-mediated coexistence in this region

the mixed layer depth in the model is constant, the model admits a supercritical Hopf bifurcation of E_3. As well, we show that there are subsequent period doubling bifurcations of the resulting orbitally asymptotically stable periodic orbit, as parameter m_2 is varied, eventually leading to what appears to be chaotic dynamics. Boushaba and Pascual discussed the Hopf bifurcation, but did not find the subsequent bifurcations. We also investigate how variation in the depth of the water layer due to seasonal variation can result in an echo bloom, but not for the parameter values they claimed.

4.1 Illustration of the cases in Table 1 and competitor-mediated coexistence

We use the form for $U(N)$ given in (6) and for $G(P, T)$ described in (5). Using these forms the model we investigate is given by:

$$\dot{P} = \mu_1 P \frac{\ln(I_s + I_{in}) - \ln(I_s + I_{out})}{(k_{bg} + k_1 P + k_2 T)H} \left(\frac{N}{K + N}\right) - m_1 P \tag{24a}$$

$$\dot{T} = \mu_2 T \frac{\ln(I_s + I_{in}) - \ln(I_s + I_{out})}{(k_{bg} + k_1 P + k_2 T)H} - m_2 T \tag{24b}$$

$$\dot{N} = D_H(N^0 - N) - \mu_1 P \frac{\ln(I_s + I_{in}) - \ln(I_s + I_{out})}{(k_{bg} + k_1 P + k_2 T)H} \left(\frac{N}{K + N}\right)$$
$$+ \xi_1 m_1 P + \xi_2 m_2 T , \tag{24c}$$

with $I_{out} = I_{in} exp([-k_{bg} - k_1 P - k_2 T]H)$.

Table 2 Parameter values used to explore the dynamics of model (24a, 24b, 24c)

Parameter	N^0	H	D_H	I_{in}	ξ_1	ξ_2	k_1	k_2
Common Values	3	1	0.014	300	0.079	0.092	1	2

Parameter	m_1	m_2	μ_1	μ_2	I_s	k_{bg}	K	
Values Set 1	0.035	0.015–0.025	0.06	0.033	90	1.2	0.1	
Values Set 2	0.005–0.035	0.034	0.05	0.035	1	0.1	2	

That Case I occurs if m_1 and m_2 are sufficiently large is obvious. Using XPPAUT Ermentrout (2002) to carry out numerical continuation of bifurcation curves, first we give an example to show that all of the cases in Table 1 for which $G(0, 0) > e_1$ (Cases II, V, VI, and VII) can occur as the bifurcation parameter m_2 varies using the parameters in Table 2 called "Common Values" and "Set 1." We show that the remaining cases (Cases III and IV) can occur by varying m_1 using the parameters in Table 2 called "Common Values" and "Set 2." In the latter case, we also point out that in this example competitor-mediated coexistence occurs in Case IV for a small range of the parameter m_1 .

In our first numerical exploration we use the "Common Values" and "Set 1" given in Table 2 and take m_2 as the bifurcation parameter.

In the three bifurcation diagrams on the left in Fig. 1, we demonstrate that all of the cases in Table 1 for which $G(0, 0) > e_1$ can occur, simply by varying m_2, and hence indirectly e_2. In this case E_0 is always unstable and E_1 always exists, independent of the value of m_2. Case V occurs when m_2 is small, e.g. for example $m_2 = 0.015$. Then $e_2 < G(0, 0) < e_4$, E_2 is locally asymptotically stable, E_1 is unstable, and E_3 does not exist. The first transcritical bifurcation occurs when $e_2 = e_4$ and E_3 and E_2 coalesce. As m_2 continues to increase, Case VII is satisfied, when $e_4 < e_2$, and E_2 loses stability and E_3 is born and is initially locally asymptotically stable. It remains so, in this example, until m_2 increases further and there is a second transcritical bifurcation when $e_2 = e_5$. Here E_3 and E_1 coalesce. E_3 disappears as soon as m_2 increases further, so that $e_2 < e_5$ and E_1 becomes locally asymptotically stable. Now case VI is satisfied. E_1 remains locally asymptotically stable as m_2 increases further, but there is a final transcritical bifurcation when $e_2 = G(0, 0)$ where E_2 and E_0 coalesce. E_2 then disappears as m_2 increases further so that $G(0, 0) \leq e_2$ and Case II is satisfied.

In the three bifurcation diagrams on the right in Fig. 1, parameters are chosen so that $G(0, 0) > e_2$, and hence E_2 exists for all values of the bifurcation parameter m_1. The first transcritical bifurcation as m_1 increases from 0 occurs when E_1 and E_3 coalesce at $m_1 = 0.01089$ (indicated by $\square$ on the diagrams) and $e_2 = e_5$. Before this, we are in Case VI and E_0 and E_2 both exist and are unstable, E_3 does not exist, and E_1 is locally asymptotically stable. As soon as $m_1 > 0.01089$, E_1 loses its stability, and E_3 is born and is locally asymptotically stable and we have moved to Case VII. The second transcritical bifurcation involves E_0 and E_1 when $G(0, 0) = e_1$ (indicated by $\circ$ in the middle diagram). Now we have moved to in Case IV where E_1 disappears, while E_0 remains unstable, and E_3 (not involved in the bifurcation) remains stable. Finally there is the last transcritical bifurcation involving E_3 and E_2, when $e_4 = e_2$. As m_1 increases further we move into Case III. E_3 disappears and E_2 becomes locally asymptotically
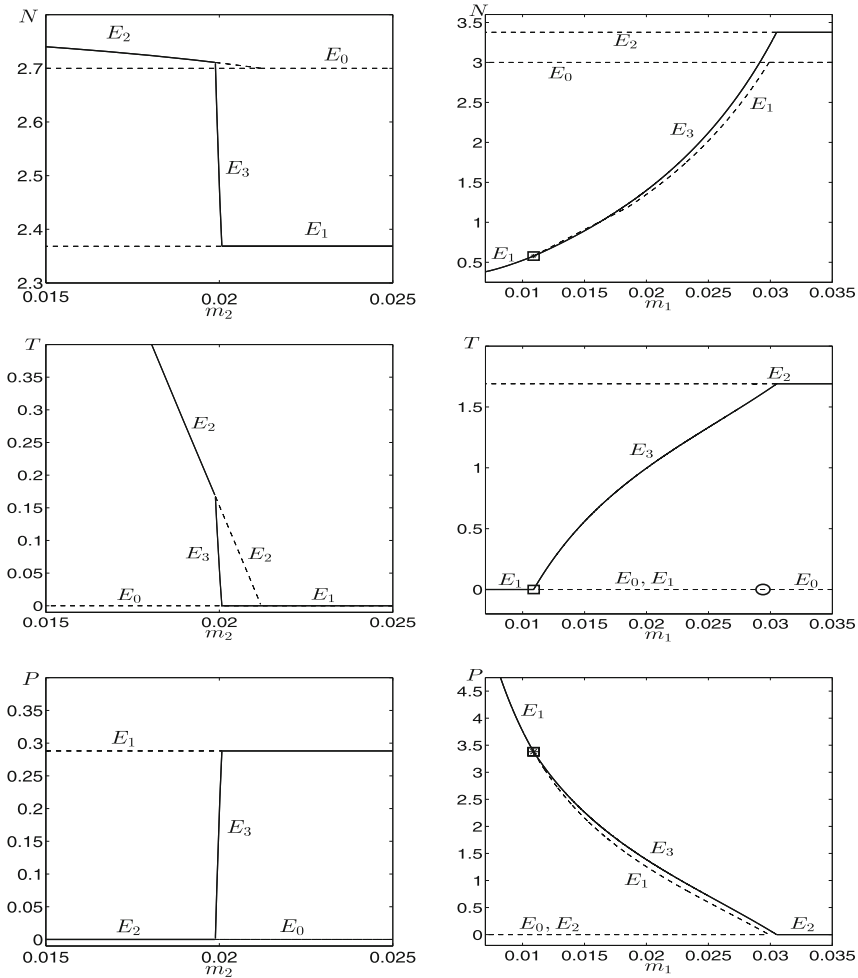
Fig. 1 *Left* Bifurcation diagrams illustrating that all of the cases in Table 1 for which $G(0, 0) > e_1$ can occur, simply by varying m_2, and hence indirectly e_2. *Right* Bifurcation diagrams illustrating a small range of parameter space near $m_1 = 0.03$ for which there is competitor-mediated coexistence, in Case IV of Table 1 where E_1 does not exist, but E_3 does. Hence, P cannot survive in the absence of T, and there is convergence to the washout equilibrium, but there coexistence with convergence to the positive equilibrium E_3 when initial conditions are positive

stable. For the small range of parameters between the second and third transcritical bifurcations, i.e., in Case IV, P cannot survive without T, but when T is present, there is uniform persistence, providing an example of competitor-mediated coexistence. In particular, when $m_1 = 0.03$, as $t \to \infty$ $(P(t), T(t), N(t)) \longrightarrow (0.0704, 1.655, 3.231)$ when the initial conditions are all positive (notice that $\lim_{t \to \infty} N(t) > 3 = N^0$), but to $(0, 0, 3)$ when $T(0) = 0$.

The stability analysis at the positive steady state E_3 (see Appendix A), shows that E_3 can only lose stability by means of a Hopf bifurcation. This would occur if the

right hand side of (27) changes sign as a parameter varies, implying that the inequality (19) does not hold. In the following numerical exploration we give an example of a Hopf bifurcation and successive period doublings.

4.2 The model of Boushaba and Pascual (2005)

The model considered in Boushaba and Pascual (2005) (see their system (12)) has the same form as our scaled model (4a, 4b, 4c), but they use specific response functions for $G(P, T)$ and $U(N)$. See Table 3 for the corresponding notation, the parameter values they used and also used here, with the interpretations they give. In fact, m_1 and m_2 would better be interpreted as the rate of loss due to mortality, sinking, and dilution.

$$
\begin{aligned}
P' &= P\left(\mu_1 \frac{\epsilon I_0}{H(t)[k_x + k_P(P+T)]}\left(\frac{N}{K+N}\right) - m_1\right) \\
T' &= T\left(\mu_2 \frac{\epsilon I_0}{H(t)[k_x + k_P(P+T)]} - m_2\right) \\
N' &= \frac{D}{H(t)}(N^0 - N) - \mu_1 P \frac{\epsilon I_0}{H(t)[k_x + k_P(P+T)]}\left(\frac{N}{K+N}\right) + \xi_1 m_1 P + \xi_2 m_2 T
\end{aligned} \tag{25}
$$

where time t is given in days, and P, T, and N have units mmol m^{-3} (millimoles per cubic meter).

4.2.1 All the cases in Table 1 occur in the model of Boushaba and Pascual

We choose m_1 and m_2 as two bifurcation parameters and use XPPAUT Ermentrout (2002) to obtain a two parameter bifurcation diagram (see Fig. 2) showing that when $\xi_2 > 0$ all cases in Table 1 occur. However, if $\xi_2 = 0$ then Case IV does not occur. Setting $\xi_1 = 0$ does not seem to make a significant difference.

4.2.2 Oscillatory and chaotic dynamics in model (25)

We consider the model of Boushaba and Pascual (25) and show that even under the assumption of constant mixed layer depth the model admits complex dynamics. We take $\mu_2 = 45.9$ and $H = 20$. Otherwise, except for the choice of m_2, we use the parameter values given in Table 3. First we provide a bifurcation diagram showing how the dynamics change as m_2 is varied (see Fig. 3). In particular, we observe a Hopf bifurcation and at least three period doubling bifurcations. Corresponding time series and orbits in the three dimensional phase plane are shown in Fig. 4, showing a stable periodic orbit and what appears to be a chaotic attractor. From the analysis in the previous sections, the system is uniformly persistent when E_3 is unstable. Therefore, as expected when E_3 is unstable, convergence is to an attractor with all components positive.
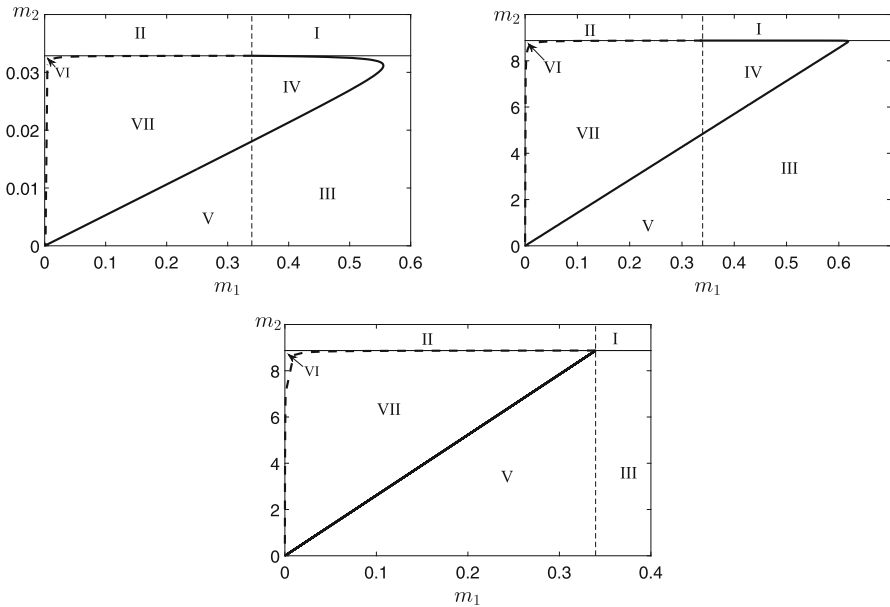
Fig. 2 *Top* Two parameter bifurcation diagram illustrating that all of the cases in Table 1 can occur for appropriate choices of the parameters m_1 and m_2 when $\xi_2 > 0$ and $H = 20$. *Left* $\mu_2 = 0.17$. *Right* $\mu_2 = 49.5$. All the other parameters are given in Table 3. *Bottom* Diagram shows the effect of setting $\xi_2 = 0$. The rest of the parameters are the same as in the *Topright* diagram. Note that region IV is no longer possible. In all of the diagrams the regions (labelled corresponding to cases) are separated by four curves: $G(0, 0) = e_1$ (*thin vertical dashed line*); $G(0, 0) = e_2$ (*thin horizontal solid line*); $e_2 = e_4$ (*thick solid curve*); and $e_2 = e_5$ (*thick dashed curve*). Of particular interest is region VII where there is uniform persistence and region IV where there is uniform persistence and competitor-mediated coexistence. Comparing the two *Top* graphs, noting the difference in the scale of the vertical axis, we see the effect of an increase in the growth rate μ_2 of T

4.2.3 "Echo blooms"

We investigate the effect of seasonal variation in water depth again using the model and parameters used in Boushaba and Pascual (2005).

As they did, we use the following function to model how the water depth changes with the seasons:

$$H(t) = \begin{cases} 200 & 0 \le t < 60 \\ 20 & 60 \le t < 270 \\ 2t - 520 & 270 \le t < 360, \end{cases} \tag{26}$$

where t is measured in days and $H(t)$ in meters. As described in Boushaba and Pascual (2005), this function approximates the three major features of the annual cycle: a rapid shallowing in spring, a constant shallow layer throughout the summer, and a deepening during the autumn and winter.

We compare the time series for three different values of μ_2: 0.17, 0.8, and 1.17, because we did not observe the echo bloom that they claimed occurs for $\mu_2 = 0.17$. However we did observe echo blooms for the other two values.

Table 3 Parameters taken from Table 1 in Boushaba and Pascual (2005), with the interpretation given there and the corresponding notation used in model (1). The same notation is used for six of the parameters

In (4a, 4b, 4c)	In Boushaba and Pascual (2005)	Description	Range	Units
N^0		Concentration of N below the mixed layer	0.6	mmol[†] m^{-3}
D		Mixing rate	0.005	m[‡] day^{-1}
H	Z	Mixed water layer depth	20–200	m
μ_1	μ_P	Maximal growth rate, P	3.22	day^{-1}
μ_2	μ_T	Maximal growth rate, T	0.17	day^{-1}
m_1	S_P	Natural mortality rate of P	0.08	day^{-1}
m_2	S_T	Natural mortality rat of T	0.09	day^{-1}
ξ_1	η	Recycling efficiency of P	0.5	Dimensionless
ξ_2	γ	Recycling efficiency of T	0.8	Dimensionless

$$G(P, T) = \frac{\epsilon I_0}{Z(k_x + k_P(P+T))} \quad \text{and} \quad U(N) = \frac{N}{N+K}$$

ϵI_0		Light efficiency at surface	0.116	Dimensionless
k_x		Shortwave extinction coefficient	0.03	m^{-1}
k_P		Phytoplankton-specific attenuation coeff.	0.0223	m^2 mmol^{-1}
K		Half saturation coefficient in $U(N)$	0.5	mmol m^{-3}

The Trichosmodium $T(t)$, seems to stimulate an "echo bloom" of the phytoplankton $P(t)$ (i.e. a secondary bloom in the summer) provided the growth rate μ_2 of $T(t)$, is large enough. When μ_2 is too small, there is no "echo bloom" [see Fig. 5 (Left)]. The larger μ_2, the larger the "echo bloom" appears to be [see Fig. 5 (Middle) and (Right)] . It seems that with a sufficiently large rate μ_2, T does not increase immediately, because it grows slowly and is out-competed for light by the non-nitrogen fixing phytoplankton P. Eventually the biomass of T begins to accumulate, but only after the spring phytoplankton bloom of P begins to crash. T then increases in the mid to late summer when the growth of P is strongly nutrient-limited. Eventually, as T blooms, the nutrient level increases due to nitrogen fixation and this stimulates the growth of P, resulting in the so-called "echo bloom" of P.
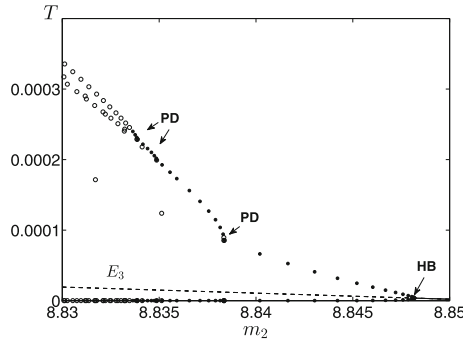
Fig. 3 Bifurcation diagram as m_2 varies for system (25) with constant mixed layer depth $H = 20$. A Hopf bifurcation and several periodic-doubling bifurcations are shown. The parameters are given in Table 3, except $\mu_2 = 45.9$. The *solid curve* indicates E_3 is stable and the *dashed curve* that it is unstable. *Open dots* indicate the maximum and minimum values of T on unstable periodic orbits and the *smaller filled dots* indicate these values on stable periodic orbits. The Hopf bifurcation near $m_2 = 8.848$ is supercritical, i.e. gives birth to a family of orbitally asymptotically stable periodic orbits that loose stability in a period doubling bifurcation near $m_2 = 8.838$. Subsequent period doubling bifurcations appear to lead to chaotic dynamics (see Fig. 4 *right*)
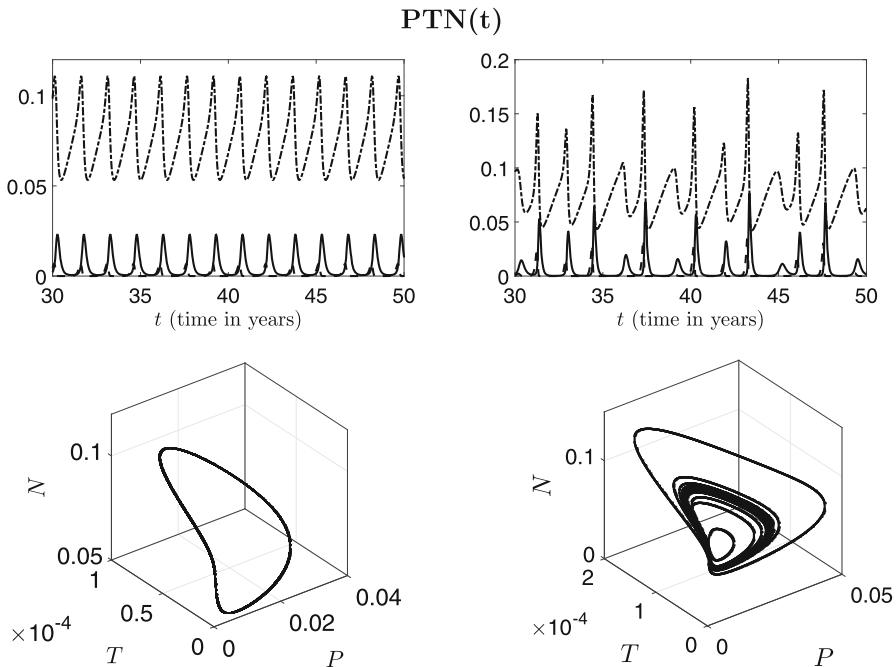

Fig. 4 *Top* Time series $P(t)$ (*thicker solid curve*), $T(t)$ (*dashed curve*), and $N(t)$ (*dash-dotted curve*), all with the scale in mmol m^{-3}. *Bottom* Orbit in the three dimensional phase plane. *Left* For $m_2 = 8.84$, convergence of the orbit is to a periodic orbit. *Right* For $m_2 = 8.83$, convergence of the orbit appears to be to a chaotic attractor. All of the other parameters are given in Table 3 except $\mu_2 = 45.9$ and $H = 20$ (as in Figs. 2 *right* and 3)
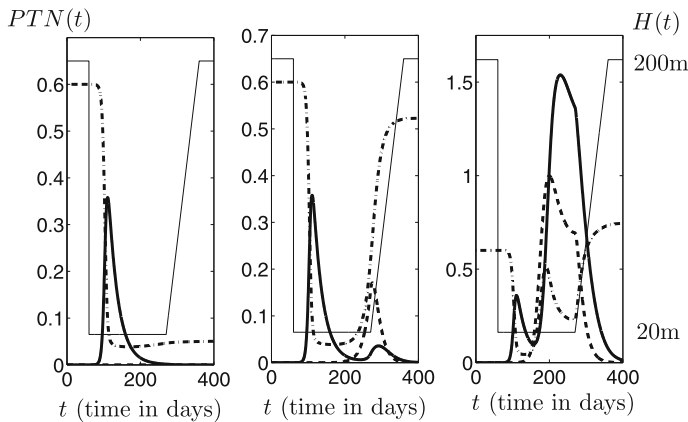
Fig. 5 Time series for system (25) with parameters taken from Table 3 in the case of seasonally fluctuating mixed layer depth modelled by $H(t)$ given by (26). Initial conditions used in all three cases were taken close to E_0 as in Boushaba and Pascual (2005): $(P(0), T(0), N(0)) = (0.0001, 0.0001, 0.6)$. Curves used: $H(t)$ (*thin solid piecewise linear curve*) with the scale in meters on the right axis; $P(t)$ (*thicker solid curve*), $T(t)$ (*dashed curve*), and $N(t)$ (*dash-dotted curve*), all with the scale in mmol m^{-3} on the left axis. Parameters used are given in Table 3. Only μ_2 differs in each graph. *Left* when $\mu_2 = 0.17$, there is no "echo bloom" for small μ_2. *Middle* $\mu_2 = 0.8$. In this case, there is a small "echo bloom" of the phytoplankton, $P(t)$, following the start of the Trichodesmium bloom $T(t)$. *Right* $\mu_2 = 1.17$. In this case, there is a large "echo bloom" of the phytoplankton, $P(t)$, again following the start of the Trichodesmium bloom $T(t)$

5 Conclusion

We considered a simplified aquatic ecosystem model involving the interaction between non-nitrogen-fixing phytoplankton and nitrogen-fixing Trichodesmium. We assumed that light is required for growth of both populations and that the non-nitrogen fixing population is also limited by nitrogen. Our model is a generalization of the model studied by Boushaba and Pascual (2005). The model captures the essential features of the ecosystem models introduced by Coles et al. (2004), Hood et al. (2001), reproducing the general characteristics of the observed Trichodesmium phytoplankton biomass distribution and can generate a secondary echo bloom when the depth of the water column is assumed to fluctuate seasonally.

We summarized our analytical results for the existence and stability of the equilibrium solutions of our general model in Table 1 and proved that there is uniform persistence of both phytoplankton populations whenever the coexistence equilibrium E_3 exists. When the recycling rate of the nitrogen fixing population T is positive, (i.e, $\xi_2 > 0$) Case IV in Table 1 can occur. In this case, there is competitor-mediated coexistence, i.e. parameters are such that P cannot survive in the absence of T, but does survive when it is present. We then showed that varying the loss rates, a sum of species specific death rates and sinking rates, moves the dynamics between the different cases. According to Table 1, it is clear that $G(0, 0)$, the local light averaged over the mixed layer of maximum depth H in the absence of all phytoplankton, plays a key role in determining which populations of phytoplankton can survive. More precisely, it is the relative values of $G(0, 0)$ and the ratios e_i that are proportional to the loss

rates m_i and inversely proportional to either the maximal growth rates or the growth rates at certain concentrations of the limiting nutrient, without the inhibitory effect of phytoplankton density.

Using numerical techniques, we also showed that even in the case that the mixed layer is assumed to have constant depth, Hopf bifurcation results in intrinsic oscillatory behavior and there are subsequent period doubling bifurcations that appear to led to chaotic dynamics. Finally we allowed the mixed layer depth to vary seasonally and showed that the maximal growth rate of the nitrogen fixing phytoplankton, Trichodesmium, μ_2, needs to be large enough in order for echo blooms to occur.

There are some obvious limitations in the model. For example, we assume that turbulent mixing is strong enough to produce a homogeneous distribution of biomass and nutrient in the mixed layer, allowing us to use a system of ordinary differential equations to model the system rather than a system of partial differential equations. We also ignore environmental conditions such as wind, that it have been demonstrated to be a driving force for promoting the growth of Trichodesmium (see Bell et al. 1999). Hence, we do not expect our simplified model to capture the precise dynamics of a real complex plankton system. However, we have demonstrated the rich dynamics and likely difficulty in predicting phytoplankton blooms that one might expect if an aquatic system includes nitrogen fixing and non-nitrogen fixing phytoplankton that both require light for growth.

Appendix A: Local stability calculations for system (4a, 4b, 4c)

Let $G_P(P, T) := \frac{\partial}{\partial P} G(P, T)$ and $G_T(P, T) := \frac{\partial}{\partial T} G(P, T)$. The Jacobian of the vector field of (4a, 4b, 4c) is given by:

$$J(P, T, N)$$
$$= \begin{bmatrix} j_{11}(P, T, N) & \mu_1 P G_T(P, T) U(N) & j_{13}(P, T, N) \\ \mu_2 T G_P(P, T) & \mu_2(G(P, T) + T G_T(P, T)) - m_2 & 0 \\ j_{31}(P, T, N) & -\mu_1 P G_T(P, T) U(N) + \xi_2 m_2 & -D_H - j_{13}(P, T, N) \end{bmatrix},$$

where $j_{ik}(P, T, N)$ denotes the ikth component of $J(P, T, N)$. In particular,

$$j_{11}(P, T, N) = \mu_1 U(N)(G(P, T) + P G_P(P, T)) - m_1$$
$$j_{13}(P, T, N) = \mu_1 P G(P, T) U'(N)$$
$$j_{31}(P, T, N) = -\mu_1 U(N)(P G_P(P, T) + G(P, T)) + \xi_1 m_1$$

Therefore, to determine the stability of the washout steady-state consider,

$$J(E_0) = \begin{bmatrix} \mu_1 G(0, 0) U(N^0) - m_1 & 0 & 0 \\ 0 & \mu_2 G(0, 0) - m_2 & 0 \\ -\mu_1 G(0, 0) U(N^0) + \xi_1 m_1 & \xi_2 m_2 & -D_H \end{bmatrix}.$$

Since the eigenvalues of this matrix lie along the diagonal, it follows that E_0 is locally asymptotically stable if $G(0, 0) < \min\left\{\dfrac{m_1}{\mu_1 U(N^0)}, \dfrac{m_2}{\mu_2}\right\}$, and unstable when the inequality is reversed.

Next we consider the stability of E_1.

$$J(E_1) = \begin{bmatrix} j_{11}(P_1^*, 0, N_1^*) & \mu_1 P_1^* G_T(P_1^*, 0)U(N_1^*) & \mu_1 P_1^* G(P_1^*, 0)U'(N_1^*) \\ 0 & \mu_2 G(P_1^*, 0) - m_2 & 0 \\ j_{31}(P_1^*, 0, N_1^*) & j_{32}(P_1^*, 0, N_1^*) & -D_H - \mu_1 P_1^* G(P_1^*, 0)U'(N_1^*) \end{bmatrix},$$

where

$$j_{11}(P_1^*, 0, N_1^*) = \mu_1 P_1^* U(N_1^*) G_P(P_1^*, 0) < 0,$$
$$j_{31}(P_1^*, 0, N_1^*) = -\mu_1 U(N_1^*)(P_1^* G_P(P_1^*, 0) + G(P_1^*, 0)) + \xi_1 m_1$$
$$j_{32}(P_1^*, 0, N_1^*) = -\mu_1 P_1^* G_T(P_1^*, 0)U(N_1^*) + \xi_2 m_2$$

The eigenvalues of $J(E_1)$ are given by the roots of the characteristic equation,

$$\Delta = (\mu_2 G(P_1^*, 0) - m_2 - \lambda)(\lambda^2 + a_1\lambda + a_0) = 0.$$

where $a_1 = D_H + \mu_1 P_1^* G(P_1^*, 0)U'(N_1^*) - j_{11}(P_1^*, 0, N_1^*) > 0$, since $j_{11}(P_1^*, 0, N_1^*) < 0$, and

$$\begin{aligned} a_0 &= -j_{11}(P_1^*, 0, N_1^*)(D_H + \mu_1 P_1^* G(P_1^*, 0)U'(N_1^*)) \\ &\quad - j_{31}(P_1^*, 0, N_1^*)\mu_1 P_1^* G(P_1^*, 0)U'(N_1^*) \\ &= -\mu_1 P_1^* G(P_1^*, 0)U'(N_1^*)(j_{11}(P_1^*, 0, N_1^*) + j_{31}(P_1^*, 0, N_1^*)) \\ &\quad - j_{11}(P_1^*, 0, N_1^*)D_H \\ &= -\mu_1 P_1^* G(P_1^*, 0)U'(N_1^*)(-\mu_1 G(P_1^*, 0)U(N_1^*) + \xi_1 m_1) - j_{11}(P_1^*, 0, N_1^*)D_H \\ &= \mu_1 P_1^* G(P_1^*, 0)U'(N_1^*)(1 - \xi_1)m_1 - j_{11}(P_1^*, 0, N_1^*)D_H > 0, \end{aligned}$$

using the fact that at E_1, $m_1 = \mu_1 G(P_1^*, 0)U(N_1^*)$. Therefore, by the Routh-Hurwicz criterion, both roots of the quadratic term have negative real parts. Hence, when E_1 exists, i.e. when (7) holds, then it is asymptotically stable when $G(P_1^*, 0) < \dfrac{m_2}{\mu_2}$, and unstable if this inequality is reversed.

Now, consider the stability of E_2.

$$J(E_2) = \begin{bmatrix} \mu_1 G(0, T_2^*)U(N_2^*) - m_1 & 0 & 0 \\ \mu_2 T_2^* G_P(0, T_2^*) & \mu_2 T_2^* G_T(0, T_2^*) & 0 \\ -\mu_1 G(0, T_2^*)U(N_2^*) + \xi_1 m_1 & \xi_2 m_2 & -D_H \end{bmatrix}.$$ The eigenvalues lie upon the diagonal of this lower triangular matrix. Since $G_T < 0$, two of them are always negative. Therefore, when E_2 exists, i.e. (11) holds, then it is locally asymptotically stable if $\mu_1 G(0, T_2^*)U(N_2^*) - m_1 < 0$, and unstable when this inequality is reversed.

Finally we consider the stability of E_3. Recall that in this case, $U(N^*) = \xi$ and $G(P^*, T^*) = \dfrac{m_2}{\mu_2}$. Consider

$$J(E_3) = \begin{bmatrix} \frac{\mu_2 m_1}{m_2} P^* G_P(P^*, T^*) & \frac{\mu_2 m_1}{m_2} P^* G_T(P^*, T^*) & \frac{\mu_1 m_2}{\mu_2} P^* U'(N^*) \\ \mu_2 T^* G_P(P^*, T^*) & \mu_2 T^* G_T(P^*, T^*) & 0 \\ j_{31}(P^*, T^*, N^*) & -\frac{\mu_2 m_1}{m_2} P^* G_T(P^*, T^*) + \xi_2 m_2 & -D_H - \frac{\mu_1 m_2}{\mu_2} P^* U'(N^*) \end{bmatrix},$$

where

$$j_{31}(P^*, T^*, N^*) = -(1 - \xi_1)m_1 - \frac{\mu_2 m_1}{m_2} P^* G_P(P^*, T^*).$$

The characteristic equation is a 3rd-order polynomial of the form

$$\Delta(\lambda) = \lambda^3 + d_2\lambda^2 + d_1\lambda + d_0 = 0,$$

where with the help of the software package Maple,

$$d_0 = -\mu_1 m_2 T^* P^* U'(N^*) \left[m_2 \xi_2 G_P(P^*, T^*) + m_1(1 - \xi_1) G_T(P^*, T^*) \right] > 0,$$

$$d_1 = -\frac{1}{\mu_2 m_2} \left[m_2 \mu_2 T^* G_T(P^*, T^*)(P^* U'(N^*)m_2\mu_1 + D_H\mu_2) \right.$$
$$\left. + P^* G_P(P^*, T^*) D_H m_1 \mu_2^2 - (1 - \xi_1)m_1 m_2^2 \mu_1 P^* U'(N^*) \right] > 0,$$

$$d_2 = \frac{1}{\mu_2 m_2} \left[-\mu_2^2(m_1 P^* G_P(P^*, T*) + m_2 T^* G_T(P^*, T*)) \right.$$
$$\left. + m_2(m_2\mu_1 P^* U'(N^*) + \mu_2 D_H) \right] > 0.$$

By the Routh-Hurwicz criterion, all roots of $\Delta(\lambda) = 0$ have negative real parts if and only if in addition $d_1 d_2 - d_0 > 0$.

$$d_1 d_2 - d_0$$
$$= \frac{1}{\mu_2^2 m_2^2} \left[G_P(P^*, T^*) P^* U'(N^*) m_2^2 \mu_1 \mu_2^2 \right.$$
$$\times \left\{ T^* m_2^2 \xi_2 - P^* m_1^2(1 - \xi_1) - P^* D_H m_1 \right\}$$
$$+ G_P(P^*, T^*) G_T(P^*, T^*) P^{*^2} T^* U'(N^*) m_1 m_2^2 \mu_1 \mu_2^3$$
$$+ D_H P^{*^2} G_P^2(P^*, T^*) m_1^2 \mu_2^4 + 2 D_H G_P(P^*, T^*) G_T(P^*, T^*) P^* T^* m_1 m_2 \mu_2^4$$
$$+ D_H G_T^2(P^*, T^*) T^{*^2} m_2^2 \mu_2^4 - G_T(P^*, T^*) P^{*^2} T^* (U'(N^*))^2 m_2^4 \mu_1^2 \mu_2$$
$$+ P^{*^2}(U'(N^*))^2 m_1 m_2^4 \mu_1^2(1 - \xi_1) - 2 D_H G_T(P^*, T^*) P^* T^* U'(N^*) m_2^3 \mu_1 \mu_2^2$$
$$+ D_H P^* U'(N^*) m_1 m_2^3 \mu_1 \mu_2(1 - \xi_1) - D_H^2 G_P(P^*, T^*) P^* m_1 m_2 \mu_2^3$$
$$- D_H^2 G_T(P^*, T^*) T^* m_2^2 \mu_2^3 + G_T^2(P^*, T^*) P^* T^{*^2} U'(N^*) m_2^3 \mu_1 \mu_2^3 \right]. \tag{27}$$

Note that all the terms in $d_1 d_2 - d_0$ are positive except the term related to the first one in the curly brackets. If the term in curly brackets is less than or equal to zero, then

$d_1 d_2 - d_0 > 0$. If $\xi_2 = 0$, this is always the case. If $\xi_2 > 0$, we explore this further, considering the two cases in Theorem 5 separately.

In case 1., $N^* \leq N^0$, and $P^* = (m_2 \xi_2 T^* + D_H(N^0 - N^*))/(m_1(1 - \xi_1))$. Substituting this for P^* in the term in curly brackets yields,

$$- \left\{ m_2 \xi_2 T^* \left((m_1 - m_2) + \frac{D_H}{1 - \xi_1} \right) + D_H(N^0 - N^*) \left(m_1 + \frac{D_H}{1 - \xi_1} \right) \right\}.$$

Therefore, in this case

$$(m_1 - m_2)(1 - \xi_1) + D_H \geq 0, \tag{28}$$

is sufficient to ensure the local asymptotic stability of E_3.

In case 2. of Theorem 5, $N^* \geq N^0$, and $T^* = (P^* m_1(1 - \xi_1) + D_H(N^* - N^0))/(m_2 \xi_2)$. Substituting this for T^* in the term in curly brackets yields,

$$- \left\{ m_1 P^*((m_1 - m_2)(1 - \xi_1) + D_H) + D_H m_2(N^* - N^0) \right\}.$$

Again, it follows that (28) is sufficient to ensure that $d_1 d_2 - d_0 > 0$, and hence E_3 is locally asymptotically stable when (28) holds.

Appendix B: Proof (5) satisfies A(i)

Proof It is easy to see that $G(P, T) > 0$ and $\lim_{P \to \infty} G(P, 0) = 0$, $\lim_{T \to \infty} G(0, T) = 0$. First we show that to prove that $\frac{\partial G}{\partial P} < 0$ and $\frac{\partial G}{\partial T} < 0$, it is equivalent to prove that $F'(x) < 0$ where

$$F(x) = \frac{-\ln(1 + A(e^{-x} - 1))}{x},$$

$0 < A = \frac{I_{in}}{I_s + I_{in}} < 1$ is a constant, and $x = (k_{bg} + k_1 P + k_2 T)H$. In fact,

$$G(P, T) = \frac{\ln \left(\frac{I_s + I_{in}}{I_s + I_{in} e^{-x}} \right)}{x} = \frac{\ln \left(\frac{1}{1 + \frac{I_{in}}{I_s + I_{in}} (e^{-x} - 1)} \right)}{x}$$

$$= \frac{-\ln(1 + A(e^{-x} - 1))}{x} = F(x),$$

and so $0 < 1 + A(e^{-x} - 1) < 1$. Therefore,

$$\frac{\partial G}{\partial P} = F'(x) \frac{\partial x}{\partial P} = k_1 H F'(x) \quad \text{and} \quad \frac{\partial G}{\partial T} = F'(x) \frac{\partial x}{\partial T} = k_2 H F'(x).$$

Since k_1, k_2, and H are all positive constants, it follows that, if $F'(x) < 0$ for $x > 0$, then $\dfrac{\partial G}{\partial P} < 0$ and $\dfrac{\partial G}{\partial T} < 0$ for $P \geq 0$ and $T \geq 0$.

Next, we show $F'(x) < 0$ for $x > 0$. Since

$$F'(x) = \frac{x A e^{-x} + [1 + A(e^{-x} - 1)] \ln[1 + A(e^{-x} - 1)]}{x^2(1 + A(e^{-x} - 1))},$$

and $A < 1$ implies that the denominator is positive, it is enough to show that the numerator,

$$h(x) = x A e^{-x} + [1 + A(e^{-x} - 1)] \ln[1 + A(e^{-x} - 1)] < 0.$$

Now,

$$h'(x) = -A e^{-x}\{x + \ln[1 + A(e^{-x} - 1)]\} = -A e^{-x} g(x),$$

where $g(x) = x + \ln[1 + A(e^{-x} - 1)]$. Since $h(0) = 0$, it remains to show that $h'(x) < 0$ for all $x > 0$. Since $g(0) = 0$ and $g'(x) = \dfrac{1 - A}{1 + A(e^{-x} - 1)} > 0$, because $0 < A < 1$ and $1 + A(e^{-x} - 1) > 0$, $g(x)$ is strictly increasing for all $x > 0$. Therefore, $h'(x) < 0$ for all $x > 0$, and the result follows. □

References

Agawin NSR, Rabouille S, Veldhuis MJW, Lidewij S, Hol S, van Overzee HMJ, Huisman J (2007) Competition and facilitation between unicellular nitrogen-fixing cyanobacteria and non-nitrogen-fixing phytoplankton species. Limnol Oceanogr 52(5):2233–2248

Bates NR, Michaels AF, Knap AH (1996) Seasonal and interannual variability of oceanic carbon dioxide species at the US JGOFS Bermuda Atlantic Time-series Study (BATS) site. Deep-Sea Res II 43(2–3):347–383

Bell PRF, Elmetri I, Uwins P (1999) Nitrogen fixation by *Trichodesmium* spp. in the Central and Northern Great Barrier Reef Lagoon: relative importance of the fixed-nitrogen load. Mar Ecol Prog Ser 186:119–126

Boushaba K, Pascual M (2005) Dynamics of the 'echo' effect in a phytoplankton system with nitrogen fixation. Bull Math Biol 67:487–507

Butler GJ, Freedman HI, Waltman P (1986) Uniformly persistent systems. Proc Am Math Soc 96:425–430

Chapin FS, Matson PA, Vitousek PM (2011) Principles of terrestrial ecosystem ecology. Springer, New York

Capone DG, Zehr JP, Paerl HW, Bergman B, Carpenter EJ (1997) Trichodesmium, a globally significant marine cyanobacterium. Science 276:1221–1229

Carpenter EJ, Romans K (1991) Major role of the cyanobacterium Trichodesmium in nutrient cycling in the North Atlantic Ocean. Science 254:1356–1358

Coles VJ, Hood RR, Pascual M, Capone DG (2004) Modeling the impact of Trichodesmium and nitrogen fixation in the Atlantic Ocean. J Geophys Res 109:C06007. doi:10.1029/2002JC001754

Diehl S (2002) Phytoplankton, light, and nutrients in a gradient of mixing depths: theory. Ecology 83:386–398

Edwards AM, Brindley J (1997) Oscillatory behavior in a three-component plankton population model. Dyn Stabil Syst 11:347–370

Ermentrout B (2002) Simulating, analyzing, and animating dynamical systems: a guide to XPPAUT for researchers and students. SIAM, Philadelphia

Falkowski PG (1997) Evolution of the nitrogen cycle and its influence on the biological sequestration of CO_2 in the ocean. Nature 387:272–275

Freedman HI, Waltman P (1984) Persistence in a model of three interacting predator-prey populations. Math Biosci 68:213–231

Grover JP (1997) Resource competition. Chapman & Hall, London

Gruber N, Sarmiento JL (1997) Global patterns of marine nitrogen fixation and denitrification. Glob Biogeochem Cy 11(2):235–266

Hood R, Bates NR, Capone DG, Olson DB (2001) Modeling the effect of nitrogen fixation on carbon and nitrogen fluxes at BATS. Deep Sea Res 48:1609–1648

Huisman J, Weissing FJ (1994) Light-limited growth and competition for light in well-mixed aquatic environments: an elementary model. Ecology 75:507–520

Huisman J, Weissing FJ (1995) Competition for nutrients and light in a well-mixed aquatic environments: a theoretical analysis. Am Nat 146:536–564

Hutson V, Schmitt K (1992) Permanence and the dynamics of biological systems. Math Biosci 111:1–71

Karl D, Letelier R, Hebel DV, Bird DF, Winn CD (1992) Trichodesmium blooms and new nitrogen in the North Pacific gyre. In: Carpenter E, Capone DG, Reuter JG (eds) Marine pelagic cyanobacteria: Trichodesmium and other diazotrophs. Kluwer Acad, Norwell, pp 219–237

Karl D, Letelier R, Tupas L, Dore J, Christian J, Hebel D (1997) The role of nitrogen fixation in biogeochemical cycling in the subtropical North Pacific Ocean. Nature 388:533–538

Kolokolnikov T, Ou CH, Yuan Y (2009) Phytoplankton depth profiles and their transitions near the critical sinking velocity. J Math Biol 59:105–122

Kunz TJ, Diehl S (2003) Phytoplankton, light and nutrients along a gradient of mixing depth: a field test of producer-resource theory. Freshw Biol 48:1050–1063

LaRoche J, Breitbarth E (2005) Importance of the diazotrophs as a source of new nitrogen in the ocean. J Sea Res 53:67–91

Michaels AF, Olson DB, Sarmiento JL, Ammerman J, Fanning K, Jahnke R, Knap AH, Lipschultz R, Prospero J (1996) Inputs, losses and transformations of nitrogen and phosphorus in the pelagic North Atlantic Ocean. Biogeochem 31:181–226

Monteiro F, Follows M (2009) On the interannual variability of nitrogen fixation in the subtropical gyres. J Mar Res 67:71–88

Olascoaga MJ, Idrisi N, Romanou A (2005) Biophysical isopycnic-coordinate modelling of plankton dynamics in the Arabian Sea. Ocean Model 8:55–80

Passarge J, Hol S, Escher M, Huisman J (2006) Competition for nutrients and light: stable coexistence, alternative stable states, or competitive exclusion? Ecol Monograph 76(1):57–72

Ruan S (1993) Persistence and coexistence in zooplankton-phytoplankton-nutrient models with instantaneous nutrient recycling. J Math Biol 31:633–654

Ruan S (2001) Oscillations in plankton models with nutrient recycling. J Theor Biol 208:15–26

Sambrotto RN, Savidge G, Robinson C, Boyd P, Takahashi T, Karl DM, Langdon C, Chipman D, Marra J, Codispoti L (1993) Elevated consumption of carbon relative to nitrogen in the surface ocean. Nature 363:248–250

Sarnelle O (1992) Nutrient enrichment and grazer effects on phytoplankton in lakes. Ecology 73:551–560

Stomp M, Huisman J, de Jongh F, Veraart AJ, Gerla D, Rijkeboer M, Ibelings BW, Wollenzien UI, Stal LJ (2004) Adaptive divergence in pigment composition promotes phytoplankton biodiversity. Nature 432:104–107

Vitousek PM, Howarth RW (1991) Nitrogen limitation on land and in the sea: how can it occur? Biogeochem 13:87–115

Watson S, McCauley E, Downing JA (1996) Patterns in phytoplankton taxonomic composition across temperate lakes of differing nutrient status. Limnol Oceanogr 42:487–495

Yuan Y (2012) A coupled plankton system with instantaneous and delayed predation. J Biol Dyn 6:148–165

Zhao X-Q (2003) Dynamical systems in population biology. Springer, New York